

# VECTORIZING TOWARDS MINERALISATION UNDER COVER USING GROUNDWATER GEOCHEMISTRY: AN EXAMPLE FROM THE CURNAMONA PROVINCE

Patrice de Caritat<sup>1</sup>, Dirk Kirste<sup>2</sup>, Graham Carr<sup>3</sup> & Malcolm McCulloch<sup>4</sup>

<sup>1</sup>CRC LEME, Geoscience Australia, GPO Box 378, Canberra, ACT,2601

<sup>2</sup>CRC LEME, Department of Geology, Australian National University, Canberra, ACT, 0200

<sup>3</sup>CSIRO Exploration & Mining, PO Box 136, North Ryde, NSW, 1670

<sup>4</sup>Research School of Earth Sciences, Australian National University, Canberra, ACT, 0200

## INTRODUCTION

The Broken Hill region is host to a single known supergiant Pb-Zn-Ag orebody and numerous smaller Pb-Zn-Ag, Cu-Au, Sn, W and U deposits, which occur in the Paleo- to Neoproterozoic basement outcrop regions of the Barrier, Olary and Flinders Ranges. Those areas of exposed basement have undergone mineral exploration for more than 100 years, yet additional significant mineral discoveries have been limited.

The Barrier, Olary and Flinders Ranges form the arcuate eastern, southern and western margins, respectively, of the Callabonna Sub-basin (Figure 1). The highly prospective Proterozoic basement is ~90% concealed by a blanket of Tertiary sediments and Quaternary soils up to 200 m thick. Traditional mineral exploration methods used in areas of outcrop face challenges when applied to areas of transported cover, especially where it is greater than a few meters thick, and new exploration tools are needed. Hydrogeochemistry could be one of these novel tools, and in this contribution we demonstrate its potential through the application of S, Sr and Pb isotopes.

## METHODS

We have collected about 300 groundwater samples from the Broken Hill region (Caritat *et al.* 2001, 2002, Kirste & Caritat 2002). These samples originate from both areas of outcrop in the ranges and areas of cover in the surrounding basins, which are the Callabonna Sub-basin, the Great Australian Basin (GAB), the Murray Basin and the Bancannia Trough. These samples have been analysed for a comprehensive suite of major, minor and trace elements as well as for several stable and radiogenic isotopes. Here, we will focus on a subset of these samples, for which we have obtained S, Sr and Pb isotope data.

The S isotopic composition of dissolved  $\text{SO}_4^{=}$  was obtained from 164 samples of  $\text{BaSO}_4$  precipitate. Results are reported in permil (‰)  $\delta^{34}\text{S}$  relative to V-CDT standard. The Sr isotopic composition was obtained from 38 samples analysed by multi-collector ICP-MS (some also by TIMS). Results

are reported as  $^{87}\text{Sr}/^{86}\text{Sr}$  ratios. The Pb isotopic composition of dissolved Pb was obtained from 29 samples collected as for Sr isotopes. The Pb

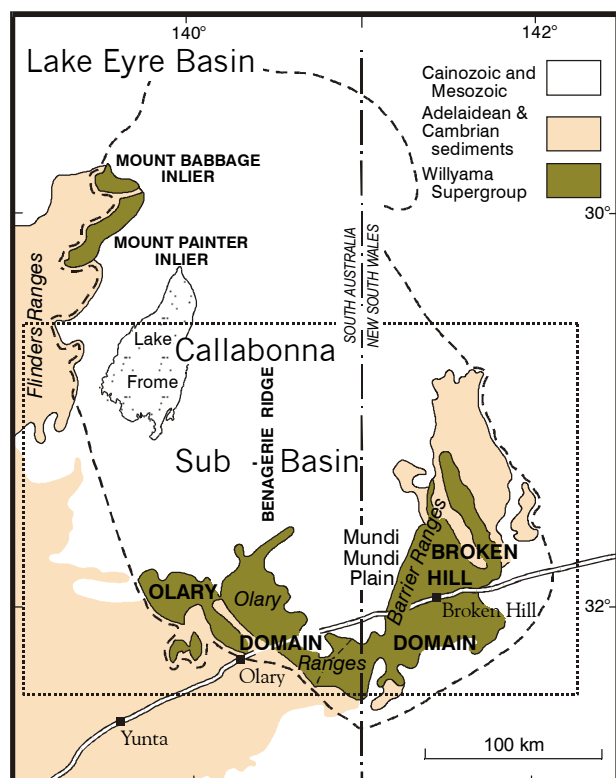
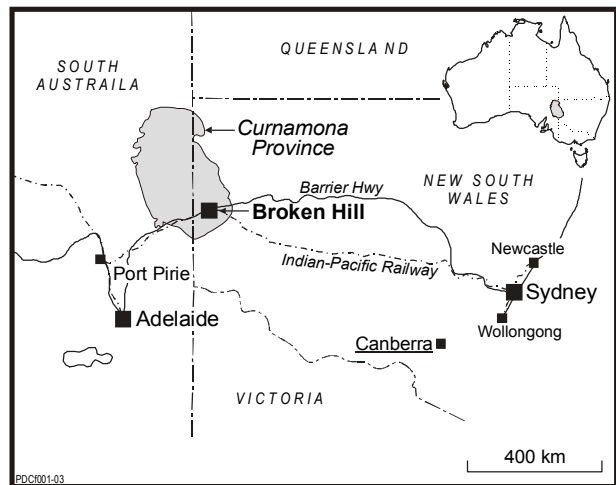


Figure 1: Location map of the study area.

was concentrated by ion exchange, then measured by TIMS. Results are reported as  $^{206}\text{Pb}/^{204}\text{Pb}$ ,  $^{207}\text{Pb}/^{204}\text{Pb}$  and  $^{208}\text{Pb}/^{204}\text{Pb}$  ratios.

## RESULTS

The isotopic compositions of the groundwaters are summarised in Table 1. Maps and scatter plots (Figs 2 and 3) illustrate the distribution of the results.

**Table 1:** Summary statistics of  $\text{SO}_4^{=}$ , Sr and Pb concentrations in groundwater and S, Sr and Pb isotopic compositions

|               | $\text{SO}_4^{=}$ | Sr       | Pb       | $\delta^{34}\text{S}$ | $^{87}\text{Sr}/^{86}\text{Sr}$ | $^{206}\text{Pb}/^{204}\text{Pb}$ | $^{207}\text{Pb}/^{204}\text{Pb}$ | $^{208}\text{Pb}/^{204}\text{Pb}$ |
|---------------|-------------------|----------|----------|-----------------------|---------------------------------|-----------------------------------|-----------------------------------|-----------------------------------|
|               | mg/L              | mg/L     | mg/L     | ‰ (V-CDT)             |                                 |                                   |                                   |                                   |
| <b>N</b>      | 164               | 149      | 164      | 159                   | 38                              | 29                                | 29                                | 29                                |
| <b>Min</b>    | <0.05             | 0.064236 | 0.0005   | 2.29                  | 0.70797                         | 16.213                            | 15.406                            | 35.898                            |
| <b>Median</b> | 864               | 3.624919 | 0.0005   | 12.71                 | 0.71949                         | 17.212                            | 15.538                            | 36.927                            |
| <b>Max</b>    | 4150              | 22.04512 | 0.013055 | 23.53                 | 0.73709                         | 18.576                            | 15.840                            | 38.397                            |

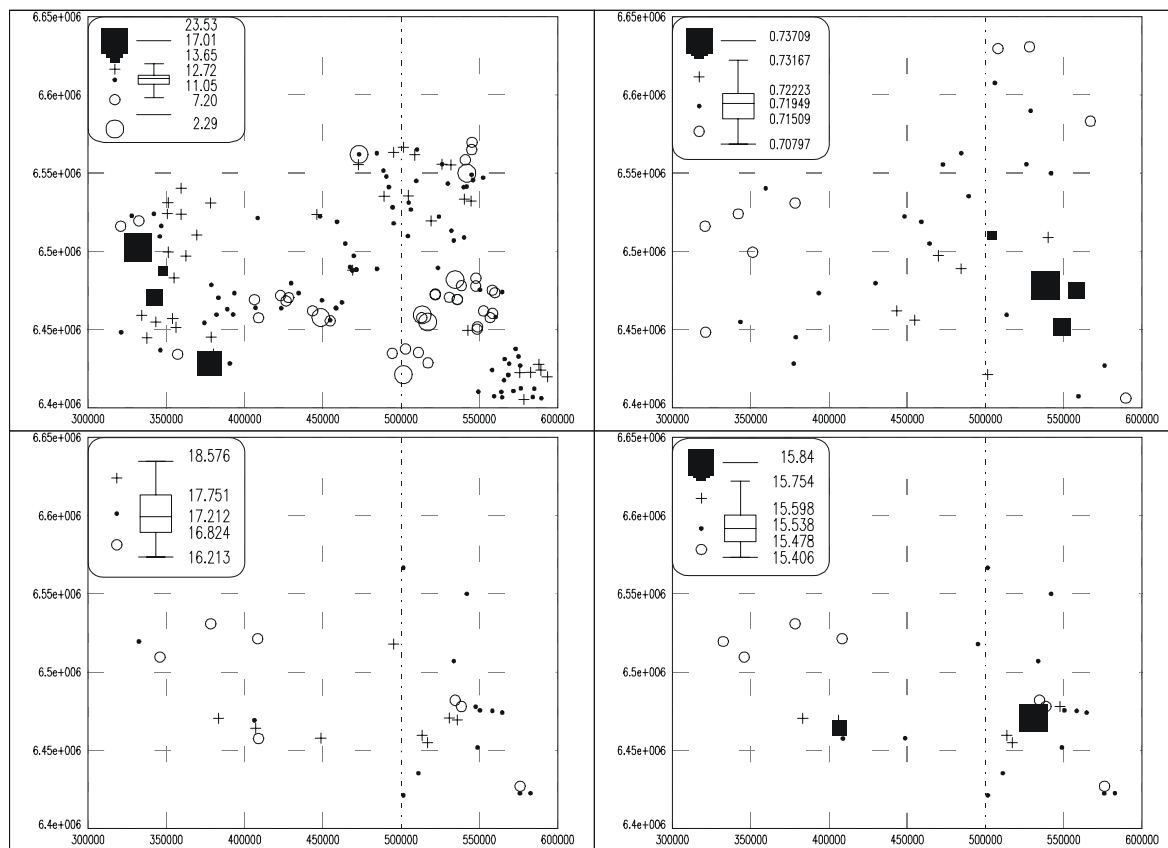
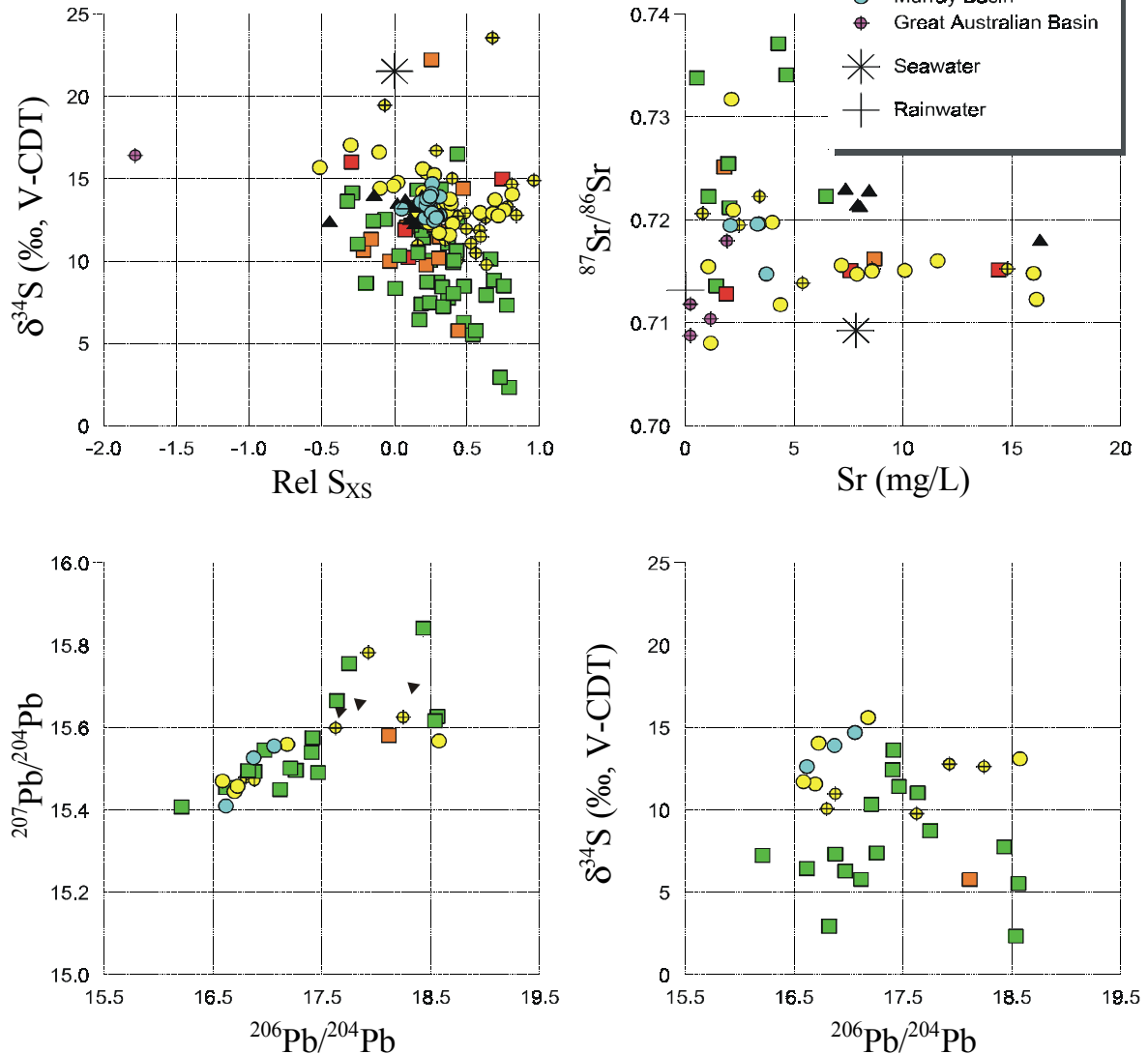


**Figure 2:** Geochemical point-source maps showing the distribution of groundwater S, Sr and Pb isotope compositions. Symbol key as per inset boxplots. Locations (top right figure) are BH: Broken Hill; FR: Flinders Ranges; OR: Olary Ranges; BR: Barrier Ranges; CSB: Callabonna Sub-basin; MB: Murray Basin; SA/NSW: South Australia-New South Wales state border. Grid 50 x 50 km; contour 200 m elevation.

## DISCUSSION AND CONCLUSIONS

The S isotopic composition of groundwater  $\text{SO}_4^{=}$  is influenced by the composition of rainfall ( $\sim +12.5$  to  $+14.5$  ‰ in the area) and the potential contribution from oxidation of sulfide minerals along the flowpath. The  $\delta^{34}\text{S}$  of Broken Hill type Pb-Zn mineralisation clusters around 0 ‰ in the Barrier Ranges and later vein mineralisation around  $+4$  to  $+7$  ‰ in the Olary Domain (Bierlein *et al.* 1996a). Figure 3a shows a plot of  $\delta^{34}\text{S}$  vs 'Relative S excess' (Rel  $S_{\text{XS}}$ ), defined as the fraction of the S concentration due neither to evaporation nor to mixing with connate water. Several groundwater samples, particularly from the ranges, have both anomalous S concentrations (Rel  $S_{\text{XS}} > 0$ ) and low  $\delta^{34}\text{S}$  compositions.

**Figure 3:** Scatter diagrams of (a)  $\delta^{34}\text{S}$  vs 'Relative S excess' (see text); (b)  $^{87}\text{Sr}/^{86}\text{Sr}$  vs Sr (seawater from Veizer 1989); (c)  $^{207}\text{Pb}/^{204}\text{Pb}$  vs  $^{206}\text{Pb}/^{204}\text{Pb}$  (ore types and growth curve from Carr & Sun 1996, Parr *et al.* 2003); (d)  $\delta^{34}\text{S}$  vs  $^{206}\text{Pb}/^{204}\text{Pb}$ .



Diagenetic pyrite in GAB sediments can have a  $\delta^{34}\text{S}$  value as low as  $-40\text{‰}$  (Chivas *et al.* 1991) and thus must be considered as a potential contributor of  $^{34}\text{S}$ -depleted  $\text{SO}_4^{2-}$  to the groundwater. There are, however, strong indications that diagenetic pyrite does not significantly influence the S-isotopic composition of the groundwaters. These include: 1) absence of trend in Figure 3a toward an end-member of composition  $-40\text{‰}$  (at  $\text{Rel S}_{\text{XS}} = 1$ ); 2) absence of trend in the  $\delta^{18}\text{O}(\text{SO}_4^{2-})$  vs  $\delta^{34}\text{S}(\text{SO}_4^{2-})$  diagram (not shown, but see Kirste *et al.* 2002) towards a diagenetic pyrite end-member; 3) the southern limit of the Bulldog Shale, a prominent formation with  $^{34}\text{S}$ -depleted diagenetic pyrite, is at the northern limit of the study area; and 4) lack of reports of abundant (if any) diagenetic pyrite (or black mudstone) in the Callabonna Sub-basin sediments. This suggests that the addition of  $^{34}\text{S}$ -depleted S we recognise in many of the groundwaters is very likely to be derived from mineralisation in the basement.

The Sr isotope results show a wide range in  $^{87}\text{Sr}/^{86}\text{Sr}$  ratios (nearly 0.0300). The majority of the values are much higher than the  $^{87}\text{Sr}/^{86}\text{Sr}$  composition of seawater during or since the Proterozoic (0.702 – 0.709; Veizer 1989). This indicates an input of radiogenic Sr through water-rock interaction dominantly through silicate hydrolysis. A plot of  $^{87}\text{Sr}/^{86}\text{Sr}$  vs Sr (Fig. 3b) indicates that there are three broad groupings: one group has  $^{87}\text{Sr}/^{86}\text{Sr}$  ratios around 0.712-0.718, another around 0.721-0.724 and the last one around 0.731-0.737. The geochemical map (Figure 2) shows that these correspond broadly to areas in the eastern, central, and southeastern regions, which roughly correlate to the interpreted basement geology and sediments derived therefrom. The less radiogenic Adelaidean rocks of the Flinders Ranges (Foden *et al.* 2001) and the more

radiogenic Willyama Supergroup rocks of the Olary and southern Barrier Ranges (Pidgeon 1967) are clearly reflected in the groundwater Sr isotopic composition.

The Pb isotope results plot along the growth curve that extends from the Broken Hill ore signature to the average background Pb signature (Fig. 3c). Those samples with the lower  $^{206}\text{Pb}/^{204}\text{Pb}$  ratios may either represent a mixing between Broken Hill type (Broken Hill Line of Lode, Pinnacles) and background signatures, or represent various other local ore types recognised in the Broken Hill district (Rupee, Sentinel, Silver King, Thackaringa, see Gulson *et al.* 1985, Bierlein *et al.* 1996b, Parr *et al.* 2003). Figure 3d shows that the samples with a low  $\delta^{34}\text{S}$  can have a wide range of  $^{206}\text{Pb}/^{204}\text{Pb}$  values (~16-18.5). All of the recharge samples with  $\delta^{34}\text{S} < 10\text{‰}$  on Figure 3d have  $\text{Rel } S_{\text{XS}} > 0$ , suggesting possible interaction with a range of different sulfide mineralisation styles as suggested by the Pb isotopic variability.

## REFERENCES

- BIERLEIN F.P., ASHLEY P.M. & SECCOMBE P.K. 1996a. *Precamb. Res.* **79**, 281-305.
- BIERLEIN F.P., HAACK U., FORSTER B. & PLIMER I.R. 1996b. *Aust. J. Earth Sci.* **43**, 177-187.
- CARITAT P. DE, KIRSTE D., DANN R. AND HUTCHEON I. 2002. In: PHILLIPS G.N. & ELY K.S. eds. *Proceedings and Field Guide, 'Victoria Undercover'*, CSIRO Publications, Collingwood, 275-278.
- CARITAT P. DE, LAVITT N. & KIRSTE D. 2001. In: CIDU R. ed., *Proc 10th Int. Symp. Water-Rock Interaction*, Balkema Pub, Swets & Zeitlinger, **Lisse 1**, 489-492.
- CARR G.R. & SUN S.S. 1996. In: PONGRATZ J. & DAVIDSON G.J. eds. *New Developments in Broken Hill Type Deposits*, CODES **Spec. Publ. 1**, 77-87.
- CHIVAS A.R., ANDREW A.S., LYONS W.B., BIRD M.I. & DONNELLY T.H. 1991. *Palaeogeog. Palaeoclim. Palaeoecol.* **84**, 309-332.
- FODEN J., BAROVICH K., JANE, M. & O'HALLORAN G., 2001. *Precamb. Res.* **106**, 291-308.
- GULSON B.L., PORRITT P.M., MIZON K.J. & BARNES R.G. 1985. *Econ. Geol.* **80**, 488-496.
- KIRSTE D. & CARITAT P. DE 2002. *Geol. Soc. Australia, Abstracts* **67**, p. 421.
- PARR J.M., STEVENS B.P.J. & CARR G.R. 2003. In: PELJO M. (comp). *BHEI Abstracts*. Geoscience Australia **Record 2003/13**, 126-129.
- PIDGEOON R.T. 1967. *J. Petrol.* **8**, 283-324.
- VEIZER J. 1989. *Ann. Rev. Earth Planet. Sci.* **17**, 141-167.

Acknowledgments: This work was funded through a Cooperative Research Centre grant and the Department of Mineral Resources New South Wales. We thank our colleagues and students for assistance with fieldwork and discussions. Landholders and mineral exploration companies granted access to the land to conduct groundwater sampling. Patrice de Caritat publishes with permission from the Chief Executive Officer, Geoscience Australia.